Title

Biochemical analysis of force-sensitive responses using a large-scale cell stretch device

Journal

Cell Adhesion & Migration, 11(5-6)

ISSN

1933-6918

Authors

Renner, Derrick J
Ewald, Makena L
Kim, Timothy
et al.

Publication Date

2017-09-03

DOI

10.1080/19336918.2016.1276147

Peer reviewed

CELL ADHESION & MIGRATION
2017, VOL. 11, NO. 5, 504–513
https://doi.org/10.1080/19336918.2016.1276147

Taylor & Francis
Taylor & Francis Group

TECHNICAL PAPER

Biochemical analysis of force-sensitive responses using a large-scale cell stretch device

Derrick J. Renner[†], Makena L. Ewald[†], Timothy Kim, and Soichiro Yamada

Biomedical Engineering Department, University of California, Davis, Davis, CA, USA

ABSTRACT

Physical force has emerged as a key regulator of tissue homeostasis, and plays an important role in embryogenesis, tissue regeneration, and disease progression. Currently, the details of protein interactions under elevated physical stress are largely missing, therefore, preventing the fundamental, molecular understanding of mechano-transduction. This is in part due to the difficulty isolating large quantities of cell lysates exposed to force-bearing conditions for biochemical analysis. We designed a simple, easy-to-fabricate, large-scale cell stretch device for the analysis of force-sensitive cell responses. Using proximal biotinylation (BioID) analysis or phospho-specific antibodies, we detected force-sensitive biochemical changes in cells exposed to prolonged cyclic substrate stretch. For example, using promiscuous biotin ligase BirA* tagged α-catenin, the biotinylation of myosin IIA increased with stretch, suggesting the close proximity of myosin IIA to α-catenin under a force bearing condition. Furthermore, using phospho-specific antibodies, Akt phosphorylation was reduced upon stretch while Src phosphorylation was unchanged. Interestingly, phosphorylation of GSK3β, a downstream effector of Akt pathway, was also reduced with stretch, while the phosphorylation of other Akt effectors was unchanged. These data suggest that the Akt-GSK3β pathway is force-sensitive. This simple cell stretch device enables biochemical analysis of force-sensitive responses and has potential to uncover molecules underlying mechano-transduction.

ARTICLE HISTORY
Received 3 August 2016
Revised 15 December 2016
Accepted 17 December 2016

KEYWORDS
α-catenin; Akt; biotin identification (BioID); force-dependent protein interactions; GSK3β; mechanotransduction; substrate stretch

Introduction

In multi-cellular organisms, individual cells are connected to neighboring cells via cell-extracellular matrix and cell-cell adhesion. This physical integration of cells is an essential feature of epithelial tissues and serves as the molecular basis of tissue architecture. Epithelial tissues, however, are not static structures. For example, epithelial cells migrate collectively during embryogenesis,[1-3] tissue regeneration,[4,5] and in some diseases like cancer,[6,7] in which adhesive contacts play a major role.[8,9] Therefore, the regulation of cell adhesion dynamics between cells or cell and extracellular matrix is paramount to physiology (and pathology) of epithelial tissues.

One of the key features of all cell junctional complexes is the ability to withstand and transmit physical forces. While the extracellular domain of adhesion proteins binds to the extracellular matrix or neighboring cells, the intracellular domain of adhesion proteins binds to cytoskeletal structures to form a unified structural network across cells and the extracellular matrix. However, this cytoskeletal linkage is not a direct molecular linkage (i.e., adhesion proteins do not directly bind to the actin cytoskeleton). Instead, numerous cytoplasmic proteins interface the intracellular domain of adhesion proteins and the cytoskeletal network, and spatial organization of some proteins in the adhesive complexes has been resolved.[10,11] These cytoskeletal linkers at cell junctions are thought to regulate the strength of and force-transmission through cell adhesion.

Interestingly, cell junctions respond to externally applied forces. The seminal study on integrin-mediated cell-extracellular matrix adhesion demonstrated that integrin junctions stiffen and recruit talin and vinculin when shear stress is applied.[12] While integrins have been known to respond to mechanical forces, recent studies have shown that the cadherin complex also responds to external mechanical forces. For example, in live cells, the application of mechanical stress stiffens cadherin junctions[13] and recruits actin[14,15] and vinculin.[15,16] In fact, cadherins appear to be under constant tension.[17] These

CONTACT Soichiro Yamada syamada@ucdavis.edu 451 Health Sciences Dr. GBSF 2317, Davis, CA 95616, USA.
[†]These authors contributed equally to this work.

studies suggest both integrin and cadherin junctions are dynamic, force-responsive molecular complexes.

Force-dependent protein recruitments at adhesive complexes are thought to be mediated by force-induced protein conformational changes that result in altered biochemical properties. For example, fibronectin, an extracellular matrix protein, assembles into fibrous structures by exposing cryptic bundling sites upon force-induced conformational change.[18] Similarly, both p130cas and talin unfold from applied force which exposes cryptic phosphorylation sites[19] and vinculin binding sites in its rod domain,[20] respectively. Furthermore, the α-catenin-vinculin interaction depends on force-generating myosin II activity,[21] and β-catenin bound α-catenin interacts with an actin filament in a force-dependent manner.[22] Recently, YAP/TAZ proteins were identified as signaling molecules for mechano-transduction.[23] While force-sensitive conformational change is not the only proposed mechanism for force-sensing,[24,25] the assembly of force-induced protein complexes is the driving mechanism of mechano-transduction. Yet, a list of components in the mechano-sensitive complex at adhesive contacts remains incomplete.

This is in part due to the lack of a large-scale cell culture system that can apply external strain onto cells and promote force sensitive biochemical changes. In some cases, the force-sensitive responses are indirectly inferred from the use of myosin II inhibitors to deplete cellular contractility. Alternatively, external strains are applied to adherent cells using flexible membrane substrates.[26,27] These flexible substrates are often manufactured with polydimethylsiloxane (PDMS), and stretched by a motor[28-32] or vacuum.[33-36] While several types of cell stretch devices are commercially available (e.g., Strex Inc., Flexcell International Corp., Electron Microscopy Sciences), all devices have a limited cell culture area that often optimized for microscopy analysis and are not suited to produce a large quantity of cell lysates for biochemical analysis.

We designed a simple substrate stretch device to exert strain onto adhered cells. This system is based on a thin PDMS membrane as a substrate, which stretches uni-axially and cyclically. The device is easy to fabricate from acrylic sheets and commercially available parts. We characterized the strain profile of the membrane and biochemically tested force-sensitive responses of adherent cells. This device is ideally suited for experiments that require a large quantity of cell lysates to improve the yield of low abundance proteins (e.g., signaling proteins) or for protein identification using mass spectrometry analysis.

Results

Design and fabrication of a large-scale cell stretch device

To analyze biochemical responses of cells experiencing mechanical perturbations, we designed a large-scale cell stretch device to apply strain onto cells. The principle of this cell stretch device is based on a flexible substrate that undergoes cyclic stretch, thereby applying strain onto adherent cells. The membrane is bounded at 2 sides, and clamped onto acrylic mounts (Fig. 1A and S1). The membrane is fabricated from PDMS using a mold (Fig. 1B) and is coated with extracellular matrix to promote cell adhesion. One of the membrane mounts is attached to the carriage and rail system and translated by a servo motor programmed to generate a cyclic stretch pattern (e.g., sine or triangular) with a defined amplitude and frequency (Fig. 1C). To ensure that the commanded stretch pattern is closely replicated by the device, the actual stretch pattern was recorded and analyzed (Fig. 1C). Direct comparison of commanded (line) and actual (circles) membrane stretch pattern demonstrated that the amplitude and frequency of membrane stretch were precisely controlled (Fig. 1C). Additional details of design and fabrication of this device are described in Materials and Methods.

Thickness of the PDMS membrane is a critical design parameter as too thin of a membrane will be easy to rip and too thick of a membrane will be difficult to stretch. Due to the size of the PDMS membrane (typically 19×16 cm with the cell culture area of 14×16 cm), spin coating, often used for micro-fabrication of PDMS film, produces membranes that are too thin, difficult to handle and easy to rip. Instead, we poured hexane-diluted PDMS (to reduce the viscosity and allow for easier handling) in a membrane mold while ensuring the surface was perfectly level (Fig. 1B), and cured the membrane at room temperature. This process ensures consistent thickness and reproducibility. The membrane thickness was routinely checked by weighing small membrane cutouts (see Fig. 2 for membrane characterization).

The cured PDMS membrane was cut to size, plasma cleaned, and collagen coated to promote cell adhesion. The MDCK epithelial cells rapidly adhered to the membrane surface and formed a cell monolayer. Based on our previous study using a commercially available small stretch chamber,[37] the membrane was stretched to 25% strain at a frequency of 0.3 Hz for ~20 hours. Under these conditions, the cells aligned perpendicular to the direction of stretch (Fig. 1D), a morphological response consistent with our previous study using a small stretch chamber.[37]

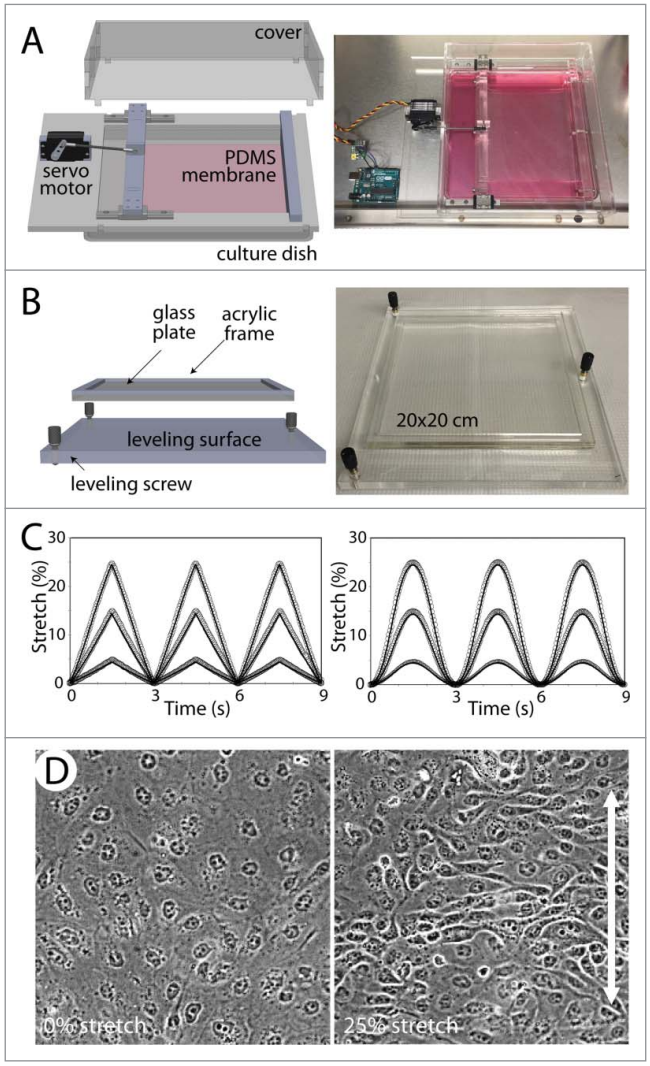

Figure 1. Design of large-scale cell stretch device and PDMS membrane mold. (A) 3D rendering (left) and actual image (right) of the large-scale cell stretch device. The device consists of a platform that houses the motor and membrane mounts, a cover, and a tissue culture dish. The membrane is mounted at 2 ends and one of the ends slides along the axis of stretch. See also Figure S1 for close-up images. (B) 3D rendering (left) and actual image (right) of the PDMS membrane mold. The membrane mold (an acrylic frame glued to a glass plate) is placed on the adjustable leveling surface. Hexane-diluted PDMS is poured onto the mold to produce a membrane with uniform thickness. (C) Triangular and sine stretch functions generated by the servo motor, which can be programmed to produce different stretch patterns with a defined frequency and amplitude of stretch. The actual displacement of sliding membrane mount (symbol) closely follows the commanded position (line). (D) Cell morphology of MDCK cells under control (left) and stretch (right) condition. In the control sample, these cells form a monolayer with cobblestone cell shape, whereas, in the stretched sample, these cells become elongated in the direction perpendicular to the stretch axis.

Characterization of PDMS membrane strain

For biochemical analysis, uniform mechanical exposure minimizes cell phenotype and biochemical variation. Since the strain heterogeneity may be an issue for large substrates, we analyzed strain distribution of the PDMS substrate. To quantify local membrane strains, fiducial markers were printed on the membrane surface, then the membrane was stretched by 25% of its initial length (Fig. 2A). As the membrane stretched, the free sides of membrane bowed inward, and consequently, generating non-zero strain values perpendicular to the stretch direction (Fig. 2A). By tracking the fiducial markers, local displacements and strains were calculated using a custom macro in ImageJ (Fig. 2B). The magnitudes of local strains averaged around 25% along the stretch axis of the membrane (Fig. 2D). This was consistent with a uniform thickness of the membrane (Fig. 2C). While the substrate near the bound edges of the membrane stretched to a lesser extent than the center regions of the membrane (Fig. 2B), only minor deviations from the overall average strain were observed (Fig. 2E), suggesting that the majority of cells will be exposed to similar membrane strains.

Biochemical analysis of stretch-dependent responses

Using a commercially available, small cell stretch chamber and proximal biotinylation (BioID) technique, our previous study has shown that the spatial proximity of α-catenin and myosin IIA changes with substrate stretch.[37] In this technique, a protein of interest (e.g., α-catenin) is tagged to a biotin ligase (BirA*, a R118G mutant of BirA) that promiscuously biotinylates surrounding proteins, and the biotinylation profiles of the control and stretch conditions are compared in Western blots analysis. Due to the small scale stretch chambers used in this previous study, the signals of biotinylated proteins in Western blots were often weak despite using a low stringent wash for the isolation of biotinylated proteins.[37] The use of low stringent wash (0.2% SDS) preserved strong protein-protein interactions thus isolating non-biotinylated proteins that complicated subsequent analysis.[37]

The substrate membrane of our large-scale cell stretch device has a cell culture area equivalent of 4 p100 dishes. MDCK epithelial cells expressing BirA*-α-catenin were plated on the membrane and stretched with a triangular cyclic stretch function (25%, 3 second cycle) for 20 hours. Under similar conditions to the small-scale experiments,[37] but using a more stringent purification protocol with 2% SDS wash to remove any non-biotinylated proteins from streptavidin beads, we purified biotinylated proteins from BirA*-α-catenin expressing cells. Both BirA*-α-catenin and β-catenin were biotinylated and the biotinylation levels were similar in the control and stretch conditions (Fig. 3A). As shown previously,[37] biotinylation of myosin IIA was significantly increased in

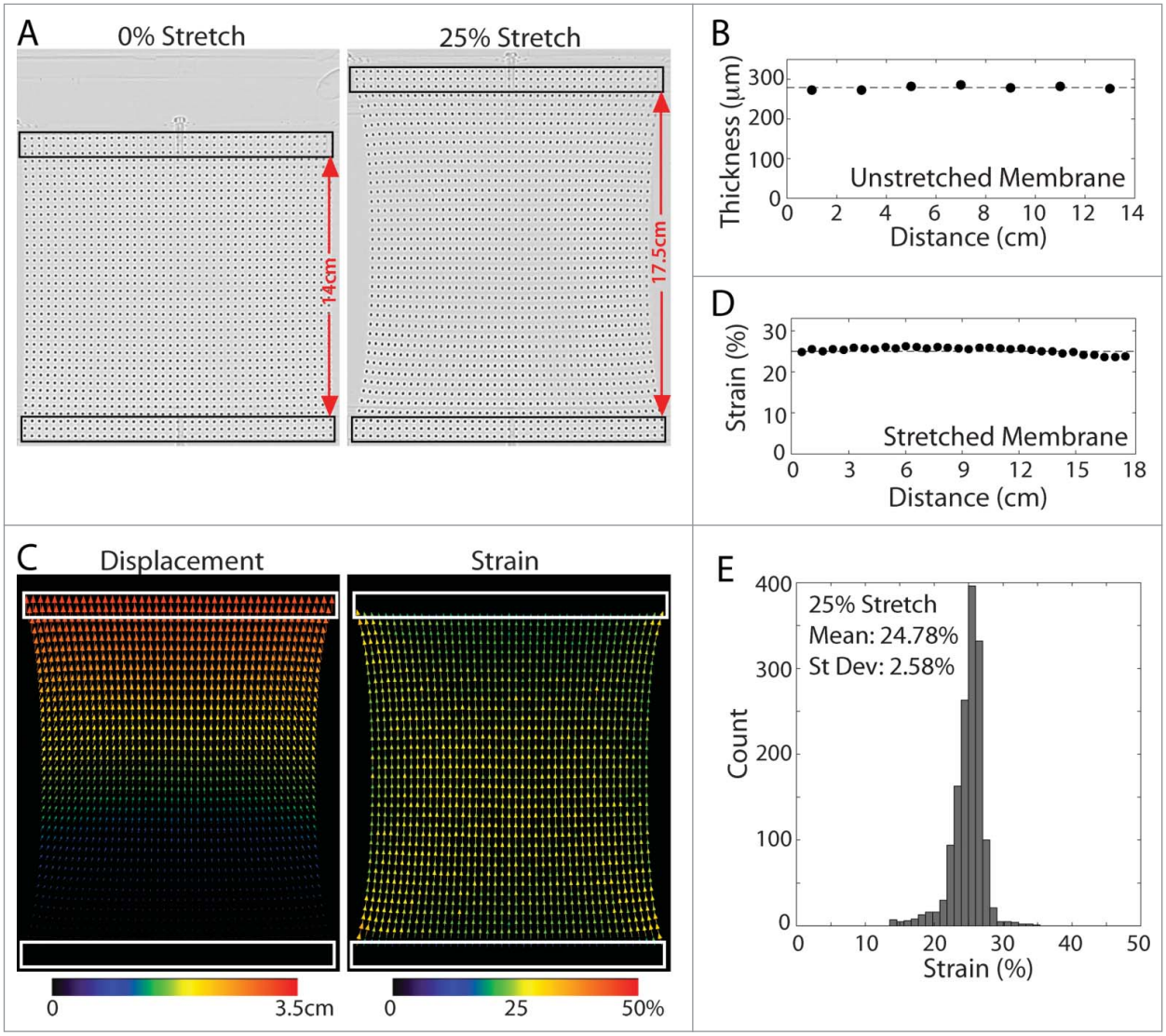

Figure 2. Characterization of PDMS-membrane strain. (A) The PDMS membrane mounted on the stretch device at 0 (left) and 25% (right) stretch. Cell culture area of PDMS membrane is 14 × 16 cm (224 cm^2, corresponds to cell attachment area equal to 4 p100 dishes) with ~0.3 mm thickness. The membrane is labeled with small black fiducial markers to track local membrane strains. The rectangular boxes denote where the membrane is mounted. (B) The thickness of PDMS membrane along the length of the membrane. The thickness was calculated based on the weight and density of PDMS. (C) The displacement (left) and strain (right) map of the membrane at 25% stretch. The magnitude and direction of the displacement and strain are indicated by pseudo-colored arrows. The rectangular boxes denote where the membrane is mounted. (D) The average strains of PDMS membrane along the stretch direction for 25% stretch. (E) Histogram of strains of PDMS membrane shown in (C).

stretch condition relative to control, while biotinylation of myosin IIB was undetectable in both control and stretch conditions (Fig. 3A). These large-scale experiments confirm the previous observation that the spatial proximity of α-catenin and myosin IIA increases in the presence of mechanical perturbation, but without any ambiguity of potential false positives from a low stringent wash condition.

To further demonstrate the utility of the large-scale cell stretch device, phosphorylation status of various signaling proteins was surveyed using commercially available, phospho-specific antibodies. Previous studies have shown that the activity of Src kinase is responsive to external mechanical forces.[38] Src proteins undergo a conformational change that promotes auto-inhibition of its kinase activity, and Y416 or Y527 phosphorylation is a proxy for Src activation or inhibition, respectively.[39] When MDCK epithelial cells were stretched with a triangular cyclic stretch function (25%, 3 second cycle, 20 hour duration), Src protein level was the same in both control and stretch cell lysate (Fig. 3B). Furthermore, the Src phosphorylation at Y416 (activating) or

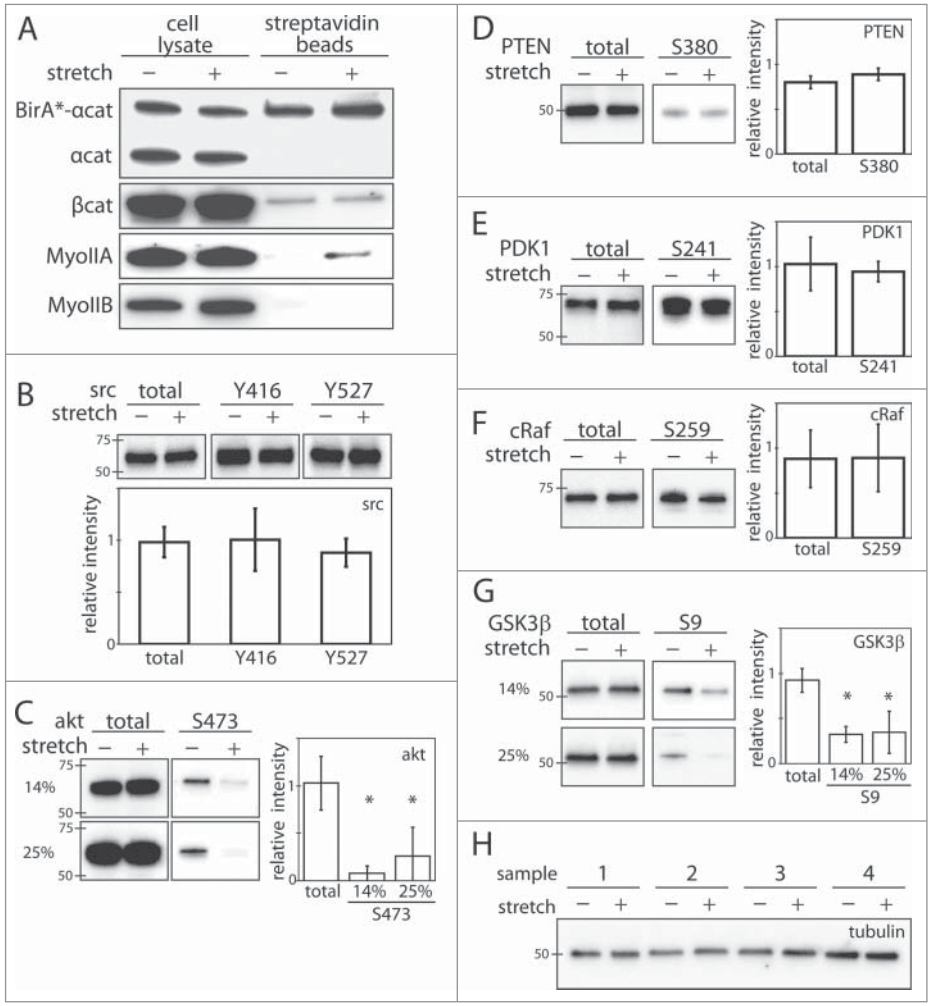

Figure 3. Biochemical analysis of force-sensitive responses. (A) Proximal biotinylation by BirA*-tagged α-catenin. Biotinylated proteins from BirA*-tagged α-catenin expressing MDCK cells were purified and analyzed using Western blots. Both BirA*-tagged α-catenin and β-catenin are biotinylated equally in both control and stretch conditions. In contrast, myosin IIA is biotinylated significantly more in stretch than control condition. Note that myosin IIB is not biotinylated by BirA*-tagged α-catenin regardless of stretch condition. (B) Src phosphorylation is stretch-independent. Cell lysates from control and stretched samples were blotted and the relative intensities (stretch/control) were quantified for total Src (n = 5, 0.98 ± 0.14) and phosphorylation specific (Y416, 1.00 ± 0.30, and Y527, 0.88 ± 0.13) antibodies (n = 5). (C) Akt phosphorylation is stretch-dependent. Cell lysates from control and stretched samples are blotted and the relative intensities (stretch/control) are quantified for total Akt (n = 4, 1.02 ± 0.28) and phosphorylation specific S473 (14%: n = 2, 0.08 ± 0.08 and 25%: n = 4, 0.26 ± 0.31) antibodies. Two different stretch conditions, 14% and 25%, are shown. All other analysis was conducted using 25% substrate stretch except GSK3β experiments shown in Fig. 3G. Results were analyzed using a one-way ANOVA; significance was determined using Dunnett's post hoc test. Results were considered significant with $P < 0.05$. (D) PTEN is an upstream effector of Akt signaling pathway. The total PTEN level (n = 3, 0.80 ± 0.07) and phosphorylation status of PTEN at S380 (n = 3, 0.88 ± 0.07) did not change with the stretch. (E) PDK1 is an upstream effector of Akt signaling pathway. The total PDK1 level (n = 3, 1.03 ± 0.30,) and phosphorylation status of PDK1 at S241 (n = 3, 0.94 ± 0.11) did not change with the stretch. (F) cRaf is a downstream effector of Akt signaling pathway. The total cRaf level (n = 3, 0.88 ± 0.32) and phosphorylation status of cRaf at S259 (n = 3, 0.89 ± 0.38) did not change with the stretch. (G) GSK3β is a downstream effector of Akt signaling pathway. While the total GSK3β level (n = 4, 0.92 ± 0.13) did not change with the stretch, the phosphorylation of GSK3β at S9 (14%: n = 2, 0.33 ± 0.09 and 25%: n = 4, 0.35 ± 0.23) decreased in the stretch lysate relative to the control lysate. Two different stretch conditions, 14% and 25%, are shown. These results were also determined to be significant using the ANOVA analysis mentioned above with a $P<0.05$. (H) Sample loading control using tubulin. In addition to quantifying the total cell lysate concentration, equivalent loading of the blot was verified using α-tubulin antibody. The average ratio of α-tubulin between control and stretch lysates was 1.11 ± 0.13. The sample numbers indicate the replicate samples used in Fig. 3B–G.

Y527 (inhibiting) sites was also the similar level in control and stretch conditions, suggesting that Src activity in MDCK cells is not dependent on triangular cyclic stretch under these conditions (Fig. 3B).

In contrast, the activity of Akt, an essential kinase for cell survival, proliferation, and cell migration pathway, is stretch-dependent. Active Akt is phosphorylated at S473.[40] While the total Akt level remained constant

regardless of substrate stretch, the phosphorylation at S473 significantly decreased with the stretch application (Fig. 3C), suggesting that Akt activity decreases with prolonged exposure to a force-bearing condition. Interestingly, the total level and the phosphorylation status of Akt upstream effectors, PTEN (S380) and PDK1 (S241) remained constant (Fig. 3D and E). The total level and phosphorylation status of Akt downstream effector cRaf (S259) also remained constant (Fig. 3F), while the phosphorylation of another Akt downstream effector, GSK3β (S9), decreased without any changes to the total level of GSK3β (Fig. 3G). Since GSK3β is an Akt substrate and GSK3β S9 phosphorylation inhibits its activity,[41] these results suggest that stretch-dependent cell signaling deactivates Akt, and as a consequence, activates GSK3β.

Interestingly, the lower level of substrate stretch (14%) also decreased the phosphorylation of Akt at S473 and GSK3β at S9 similar to the level of 25% stretch (Fig. 3C and G). Thus, between 14 and 25% stretch, stretch-dependent Akt or GSK3β phosphorylation was not strongly dependent on the magnitude of stretch. Note that all samples were loaded equally by quantifying the cell lysate concentration and as indicated by the tubulin blot (4 representative experiments from panel B-G were blotted with a tubulin antibody, Fig. 3H). These results demonstrate the large-scale cell stretch device as an ideal experimental platform to test biochemical responses as a result of mechanical perturbations.

Discussion

Force-sensitive protein interactions are a key biochemical step in mechano-transduction. One method for analyzing force-sensitive protein interactions is promiscuous biotinylation by a mutant BirA* biotin ligase, which labels proximal proteins in live cells. A stretch device can be used to apply force-bearing conditions to the BirA* expressing cells and the difference in biotinylation patterns of control and force-bearing conditions identifies potential force-sensitive interactions.[37] Unfortunately, biotinylated proteins are often low-abundance. Due to the limited quantity of cell lysates obtained from small-scale, stretch devices, force-dependent biochemical analysis using proximal biotinylation has been inherently difficult despite a highly-efficient streptavidin purification protocol.

We designed an easy-to-fabricate, large-scale cell stretch device to probe force-sensitive biochemical responses of an epithelial cell monolayer. This device yields a quantity of cell lysates similar to traditional biochemical preparations, thus providing opportunities to analyze force-sensitive, low abundance proteins. This large-scale stretch device overcomes the sample limitation in proximal biotinylation analysis, as demonstrated by the detection of force-sensitive interaction between α-catenin and myosin IIA (Fig. 3A). Furthermore, to identify a comprehensive list of proximal proteins, purified biotinylated proteins can be analyzed using mass spectrometry, which often requires a micro-gram quantity of cell lysates.[42,43] This large-scale stretch chamber will aid future proteomic studies on force-sensitive protein interactions using proximal biotinylation analysis.

An additional application includes the detection of force-sensitive post-translational modifications. Previous studies have shown that the Src protein is activated with the application of external forces. The application of tagging force via a ligand-coated particle on the cell surface, for example, promotes Src activation.[38,44] In this case, Src activation is detected by its phosphorylation status[44] or an activation sensitive Fluorescence Resonance Energy Transfer (FRET) probe.[38] However, in our biochemical analysis, Src phosphorylation status remained constant regardless of substrate stretch (Fig. 3B), suggesting that mechanical perturbation by substrate stretch is not sufficient for Src activation in our model system. This stretch independent Src phosphorylation is consistent with a similar substrate stretch experiment using a small scale device,[19] suggesting that sub-cellular stimulation, and not substrate stretch that strains a whole cell body, may be responsible for Src activation.

Interestingly, Akt phosphorylation, and thus its activation, was significantly changed with the exposure to substrate stretch. The Akt signaling pathway regulates cell survival, proliferation, cell migration.[45,46] Akt phosphorylation at S473 decreased in stretch condition (Fig. 3C), suggesting that Akt-mediated signaling is inhibited upon cell stretch. Interestingly, previous studies have shown that cell stretch can lead to increase in Akt phosphorylation. For example, Akt phosphorylation increased with the applications of cyclic substrate stretch in smooth muscle cells,[47,48] cardiomyocytes,[49] mesangial cells[50] and fibroblasts.[51] While Akt activation likely depends on cell types and its context, all previous studies have used a shorter stretch time than current work. This is consistent with an observation that substrate stretch increases the insoluble pool of Akt within 10 minutes,[52] indicating that Akt is membrane bound and activated. In smooth muscle cells, the initial increase in Akt phosphorylation, however, peaked at 6 hours and started to decline,[48] consistent with this study (Fig. 3C). These studies highlight the diverse roles of the Akt signaling pathway and demonstrate force-induced signaling regulation strongly depends on time scale.

Furthermore, PTEN, PDK1 and cRaf phosphorylation status did not change while their total protein levels also remained constant (Fig. 3D-F). In contrast, GSK3β phosphorylation at S9 decreased (Fig. 3G), suggesting that

GSK3β is a down-stream effector of the force-sensitive Akt signaling pathway. Interestingly, in air-way smooth muscle cells, the application of stretch decreases the level of GSK3β by microRNA-26a,[53] demonstrating an alternative pathway to regulate GSK3β in a force-dependent manner. Furthermore, substrate stretch has been shown to activate cell proliferation mediated by Yap1 and β-catenin.[54] While GSK3β phosphorylates β-catenin in epithelial cells for degradation,[41] how GSK3β activity changes β-catenin's nuclear translocation upon stretch is unclear and may be a critical force-sensitive function of GSK3β.

Force-sensitive regulation of signaling pathways emerged as a key regulator of cell behavior due, in part, to innovative tools to probe single cell force responses (using optical tweezer, atomic force microscopy, and FRET based protein activity/conformation sensors). These tools are indispensable for detecting rapid force-initiated responses. In contrast, the use of cell stretch devices with *in situ* proximal biotinylation can detect spatial proximity of proteins under force-bearing conditions. Furthermore, biochemical analysis of cell lysates obtained from stretch devices detects long-lasting, force-sensitive responses that alter cell phenotype. In addition to signaling molecules described here, previous studies have shown that the activation of ERK signaling is responsive to mechanical stretch.[55-57] There are undoubtedly other force-sensitive signaling molecules to be discovered. With the ease of collecting concentrated cell lysates exposed to cyclic mechanical strain, this large-scale stretch device is an ideal platform to identify other force-sensitive signaling pathway. Therefore, the device outlined in this study has a wide range of applications in force-sensitive responses, and the potential to identify the molecules responsible for mechanotransduction.

Materials and methods

Design and construction of cell stretch device

The cell stretch device is based on an acrylic-based platform, a thin polydimethylsiloxane (PDMS) membrane as a substrate and a BioAssay dish (24.5×24.5 cm, Corning, Inc.) as a tissue culture dish (Figure S1A). This easy-to-fabricate cell stretch device requires minimal fabrication as acrylic sheets can be easily and precisely cut using a laser cutter (readily accessible through university facilities or private companies), constructed with a minimal number of screws and a fast-setting acrylic cement (TAP Plastics). The servo motor is mounted on the platform using an acrylic motor mount glued to the platform (Figure S1B). The membrane is bounded at opposing sides by a sliding and a fixed mount using a simple clamp system (Figure S1C and D). While the stationary membrane clamp is glued to the base acrylic frame, the sliding clamp is mounted to a carriage and rail system (McMaster-Carr) and is connected to a servo motor (Hitec RCD, Inc.) via a threaded shaft (Tamiya, Inc.). A cover was similarly assembled using acrylic sheets. All acrylic sheets were purchased from McMaster Carr and were laser cut at the in-house prototyping facility using Kern Micro 24 system (Kern Lasers Systems).

The servo motor uni-axially and cyclically displaced the sliding membrane mount to stretch the PDMS membrane. The PDMS membrane with the initial length of 14 cm was stretched to 17.5 cm (25%) or 16 cm (14%) at a frequency of 3 seconds per cycle. The servo motor was controlled by a Micro Maestro RC servo controller (Pololu Corp) and an Arduino Uno micro-controller, which were programmed using the Maestro servo software and Arduino software. The servo motor was powered by a variable power supply (9316PS, Marlin P. Jones & Assoc. Inc.).

PDMS membrane fabrication and characterization

To fabricate consistently uniform PDMS membranes, we designed a membrane mold using a borosilicate glass plate (McMaster-Carr) as a base and a laser cut acrylic as a frame. A 2-part epoxy (JB Weld) or PDMS was used to adhere the acrylic frame to the glass base. To ensure that the mold is perfectly level, a leveling platform was constructed with 3 fine-adjustment thumb screws (McMaster-Carr) as adjustable feet for the platform. The platform was leveled using a high-precision level (Geier and Bluhm) and the fine-adjustment thumb screws. Two parts PDMS is mixed at 1:10 ratio (total 15 g) then diluted in an equal volume of hexane. The diluted PDMS solution was poured onto a membrane mold on the leveling surface, and was cured at room temperature.

To monitor the movement of sliding mount, time-lapse movies were taken with a cell phone camera, and the movement was analyzed using ImageJ (see Fig. 1C). To quantify the strain profile of the PDMS membrane, fiducial markers were painted onto the membrane using a black spray paint and a transparency mask with a grid pattern consisting of 2 mm diameter circular holes that are 4 mm apart. ImageJ and a custom macro were used to quantify the strain distribution of the membrane by tracking the movement of the dots as the membrane was stretched from 0% to 25%. The strain was calculated based on the initial (ΔL_0) and final (ΔL) spacing between the markers: $\Delta L / \Delta L_0 - 1$.

Purification of biotinylated proteins and western blot analysis

The purification of biotinylated proteins was described previously.[37,43] Briefly, 30 × 10^6 cells were seeded on

large-scale cell stretch chambers and cultured for 24 hours in a DMEM media. Subsequently, biotin was added resulting in a biotin concentration of 50 μM and the membrane was stretched overnight. The control, non-stretch condition was treated identically except the motor was not powered. After 20–24 hours, the cells were washed 3 times with PBS buffer. Next, cells were lysed in BioID lysis buffer[43] supplemented with cOmplete™ Protease Inhibitor Cocktail (Roche) and PhosSTOP (Roche), then sonicated and centrifuged to isolate the supernatant. The protein concentration of the supernatant was measured with a RC/DC assay kit (Bio-Rad). Equal concentrations of lysate were added to BioMag streptavidin beads (Qiagen) and incubated overnight. Lysates were then washed with 2% SDS buffer. Finally, biotinylated proteins were eluted with a sample buffer containing 3 mM biotin and boiled for 15 minutes.

The cell lysates from control and stretch conditions were also used in the phosphorylation analysis of Src and Akt. Based on the cell lysate concentrations quantified by the RC/DC assay, the same amount of cell lysates was loaded in each lane. The equal sample loading was also verified using Ponceau staining and anti-α-tubulin blot (Fig. 3H).

For western blot applications, primary antibodies used for proximal biotinylation include: αE-catenin (15D9, Alexis Biochemical), β-catenin (Clone 14, BD Biosciences), non-muscle myosin IIA (Rabbit Polyclonal, Sigma), and non-muscle myosin IIB (Rabbit Polyclonal, Sigma). Primary antibodies used in Src signaling pathway analysis include: Src (32G6), Phospho-Src Tyr416 (mAb 6943) and Phospho-Src Tyr527 (Ab 2105). Primary antibodies used in Akt signaling pathway analysis include: pan Akt (mAb 4691), Phospho-Akt Ser473 (mAb 4060), total cRaf (D4B3J), Phospho-c-Raf Ser259 (Ab 9421), total GSK-3β (D5C5Z), Phospho-GSK-3β Ser9 (mAb 5558), total PTEN (D4.3), Phospho-PTEN Ser380 (Ab 9551), total PDK1 and Phospho-PDK1 Ser241 (mAb 3438). All Akt and Src signaling antibodies were purchased from Cell Signaling. As a loading control, the samples were analyzed using α-tubulin (DM1α, Sigma). The signals on the nitrocellulose membrane were detected using a WesternBright Quantum Chemiluminescence Kit (Advansta).

Disclosure of potential conflicts of interest

No potential conflicts of interest were disclosed.

Acknowledgments

We thank Steven Lucero for his advice and help with the design and use of UC Davis Biomedical Engineering TEAM facility and Katherine Macway and Xenia Ivanova for their contributions during the early stage of this work.

Funding

This work was supported by NIH EUREKA GM094798, UC Davis Bridge Fund, NIH R03 EB021636 and NSF 1562095 (all to SY).

References

[1] Keller R. Shaping the vertebrate body plan by polarized embryonic cell movements. Science 2002; 298:1950-4; PMID:12471247; https://doi.org/10.1126/science.1079478

[2] Weijer CJ. Collective cell migration in development. J Cell Sci 2009; 122:3215-23; PMID:19726631; https://doi.org/10.1242/jcs.036517

[3] Scarpa E, Mayor R. Collective cell migration in development. J Cell Biol 2016; 212:143-55; PMID:26783298; https://doi.org/10.1083/jcb.201508047

[4] Radtke F, Clevers H. Self-renewal and cancer of the gut: two sides of a coin. Science 2005; 307:1904-9; PMID:15790842; https://doi.org/10.1126/science.1104815

[5] Jacinto A, Martinez-Arias A, Martin P. Mechanisms of epithelial fusion and repair. Nat Cell Biol 2001; 3:E117-23; PMID:11331897; https://doi.org/10.1038/35074643

[6] Friedl P, Wolf K. Tumour-cell invasion and migration: diversity and escape mechanisms. Nature Rev Cancer 2003; 3:362-74; PMID:12724734; https://doi.org/10.1038/nrc1075

[7] Friedl P, Gilmour D. Collective cell migration in morphogenesis, regeneration and cancer. Nat Rev Mol Cell Biol 2009; 10:445-57; PMID:19546857; https://doi.org/10.1038/nrm2720

[8] Haeger A, Wolf K, Zegers MM, Friedl P. Collective cell migration: guidance principles and hierarchies. Trends Cell Biol 2015; 25:556-66; PMID:26137890; https://doi.org/10.1016/j.tcb.2015.06.003

[9] Collins C, Nelson WJ. Running with neighbors: coordinating cell migration and cell-cell adhesion. Curr Opin Cell Biol 2015; 36:62-70; PMID:26201843; https://doi.org/10.1016/j.ceb.2015.07.004

[10] Case LB, Waterman CM. Integration of actin dynamics and cell adhesion by a three-dimensional, mechanosensitive molecular clutch. Nature Cell Biology 2015; 17:955-63; PMID:26121555; https://doi.org/10.1038/ncb3180

[11] Kanchanawong P, Shtengel G, Pasapera AM, Ramko EB, Davidson MW, Hess HF, Waterman CM. Nanoscale architecture of integrin-based cell adhesions. Nature 2010; 468:580-4; PMID:21107430; https://doi.org/10.1038/nature09621

[12] Wang N, Butler JP, Ingber DE. Mechanotransduction across the cell surface and through the cytoskeleton. Science 1993; 260:1124-7; PMID:7684161; https://doi.org/10.1126/science.7684161

[13] le Duc Q, Shi Q, Blonk I, Sonnenberg A, Wang N, Leckband D, de Rooij J. Vinculin potentiates E-cadherin mechanosensing and is recruited to actin-anchored sites within adherens junctions in a myosin II-dependent manner. J Cell Biol 2010; 189:1107-15; PMID:20584916; https://doi.org/10.1083/jcb.201001149

[14] Bard L, Boscher C, Lambert M, Mege RM, Choquet D, Thoumine O. A molecular clutch between the actin flow and N-cadherin adhesions drives growth cone migration. J Neurosci 2008; 28:5879-90; PMID:18524892; https://doi.org/10.1523/JNEUROSCI.5331-07.2008

[15] Barry AK, Tabdili H, Muhamed I, Wu J, Shashikanth N, Gomez GA, Yap AS, Gottardi CJ, de Rooij J, Wang N, et al. alpha-catenin cytomechanics-role in cadherin-dependent adhesion and mechanotransduction. J Cell Sci 2014; 127:1779-91; PMID:24522187; https://doi.org/10.1242/jcs.139014

[16] Thomas WA, Boscher C, Chu YS, Cuvelier D, Martinez-Rico C, Seddiki R, Heysch J, Ladoux B, Thiery JP, Mege RM, et al. alpha-Catenin and vinculin cooperate to promote high E-cadherin-based adhesion strength. J Biol Chem 2013; 288:4957-69; PMID:23266828; https://doi.org/10.1074/jbc.M112.403774

[17] Borghi N, Sorokina M, Shcherbakova OG, Weis WI, Pruitt BL, Nelson WJ, Dunn AR. E-cadherin is under constitutive actomyosin-generated tension that is increased at cell-cell contacts upon externally applied stretch. Proc Natl Acad Sci U S A 2012; 109:12568-73; PMID:22802638; https://doi.org/10.1073/pnas.1204390109

[18] Zhong C, Chrzanowska-Wodnicka M, Brown J, Shaub A, Belkin AM, Burridge K. Rho-mediated contractility exposes a cryptic site in fibronectin and induces fibronectin matrix assembly. J Cell Biol 1998; 141:539-51; PMID:9548730; https://doi.org/10.1083/jcb.141.2.539

[19] Sawada Y, Tamada M, Dubin-Thaler BJ, Cherniavskaya O, Sakai R, Tanaka S, Sheetz MP. Force sensing by mechanical extension of the Src family kinase substrate p130Cas. Cell 2006; 127:1015-26; PMID:17129785; https://doi.org/10.1016/j.cell.2006.09.044

[20] del Rio A, Perez-Jimenez R, Liu R, Roca-Cusachs P, Fernandez JM, Sheetz MP. Stretching single talin rod molecules activates vinculin binding. Science 2009; 323:638-41; PMID:19179532; https://doi.org/10.1126/science.1162912

[21] Yonemura S, Wada Y, Watanabe T, Nagafuchi A, Shibata M. alpha-Catenin as a tension transducer that induces adherens junction development. Nat Cell Biol 2010; 12:533-42; PMID:20453849; https://doi.org/10.1038/ncb2055

[22] Buckley CD, Tan J, Anderson KL, Hanein D, Volkmann N, Weis WI, Nelson WJ, Dunn AR. Cell adhesion. The minimal cadherin-catenin complex binds to actin filaments under force. Science 2014; 346:1254211; PMID:25359979; https://doi.org/10.1126/science.1254211

[23] Dupont S, Morsut L, Aragona M, Enzo E, Giulitti S, Cordenonsi M, Zanconato F, Le Digabel J, Forcato M, Bicciato S, et al. Role of YAP/TAZ in mechanotransduction. Nature 2011; 474:179-83; PMID:21654799; https://doi.org/10.1038/nature10137

[24] Hirata H, Sokabe M, Lim CT. Molecular mechanisms underlying the force-dependent regulation of actin-to-ECM linkage at the focal adhesions. Progress Mol Biol Translational Sci 2014; 126:135-54; PMID:25081617

[25] Vogel V, Sheetz M. Local force and geometry sensing regulate cell functions. Nat Rev Mol Cell Biol 2006; 7:265-75; PMID:16607289; https://doi.org/10.1038/nrm1890

[26] Brown TD. Techniques for mechanical stimulation of cells in vitro: a review. J Biomechanics 2000; 33:3-14; PMID:10609513; https://doi.org/10.1016/S0021-9290(99)00177-3

[27] Lei Y, Ferdous Z. Design considerations and challenges for mechanical stretch bioreactors in tissue engineering. Biotechnol Progress 2016; 32:543-53; PMID:26929197; https://doi.org/10.1002/btpr.2256

[28] Faust U, Hampe N, Rubner W, Kirchgessner N, Safran S, Hoffmann B, Merkel R. Cyclic stress at mHz frequencies aligns fibroblasts in direction of zero strain. PloS One 2011; 6:e28963; PMID:22194961; https://doi.org/10.1371/journal.pone.0028963

[29] Gerstmair A, Fois G, Innerbichler S, Dietl P, Felder E. A device for simultaneous live cell imaging during uni-axial mechanical strain or compression. J Applied Physiol 2009; 107:613-20; PMID:19498100; https://doi.org/10.1152/japplphysiol.00012.2009

[30] Imsirovic J, Wellman TJ, Mondonedo JR, Bartolak-Suki E, Suki B. Design of a novel Equi-Biaxial stretcher for live cellular and subcellular imaging. PloS One 2015; 10:e0140283; PMID:26466363; https://doi.org/10.1371/journal.pone.0140283

[31] Huang L, Mathieu PS, Helmke BP. A stretching device for high-resolution live-cell imaging. Annals Biomedical Engineering 2010; 38:1728-40; PMID:20195762; https://doi.org/10.1007/s10439-010-9968-7

[32] Shao Y, Tan X, Novitski R, Muqaddam M, List P, Williamson L, Fu J, Liu AP. Uniaxial cell stretching device for live-cell imaging of mechanosensitive cellular functions. Rev Scientific Instruments 2013; 84:114304; PMID:24289415; https://doi.org/10.1063/1.4832977

[33] Ursekar CP, Teo SK, Hirata H, Harada I, Chiam KH, Sawada Y. Design and construction of an equibiaxial cell stretching system that is improved for biochemical analysis. PloS One 2014; 9:e90665; PMID:24626190; https://doi.org/10.1371/journal.pone.0090665

[34] Sim JY, Borghi N, Ribeiro A, Sorokina M, Shcherbakova O, Ramallo D, Dunn A, Nelson WJ, Pruitt BL. Uniaxial cell stretcher enables high resolution live cell imaging. Proc Ieee Micr Elect 2012.

[35] Wang D, Xie Y, Yuan B, Xu J, Gong P, Jiang X. A stretching device for imaging real-time molecular dynamics of live cells adhering to elastic membranes on inverted microscopes during the entire process of the stretch. Integr Biol 2010; 2:288-93; PMID:20532321; https://doi.org/10.1039/b920644b

[36] Ao M, Brewer BM, Yang L, Franco Coronel OE, Hayward SW, Webb DJ, Li D. Stretching fibroblasts remodels fibronectin and alters cancer cell migration. Scientific Reports 2015; 5:8334; PMID:25660754; https://doi.org/10.1038/srep08334

[37] Ueda S, Blee AM, Macway KG, Renner DJ, Yamada S. Force dependent biotinylation of myosin IIA by alpha-catenin tagged with a promiscuous biotin ligase. PloS One 2015; 10:e0122886; PMID:25806963; https://doi.org/10.1371/journal.pone.0122886

[38] Wang Y, Botvinick EL, Zhao Y, Berns MW, Usami S, Tsien RY, Chien S. Visualizing the mechanical activation of Src. Nature 2005; 434:1040-5; PMID:15846350; https://doi.org/10.1038/nature03469

[39] Roskoski R, Jr. Src kinase regulation by phosphorylation and dephosphorylation. Biochem Biophys Res Commun

2005; 331:1-14; PMID:15845350; https://doi.org/10.1016/j.bbrc.2005.03.012

[40] Scheid MP, Woodgett JR. Unravelling the activation mechanisms of protein kinase B/Akt. FEBS Lett 2003; 546:108-12; PMID:12829245; https://doi.org/10.1016/S0014-5793(03)00562-3

[41] Cohen P, Frame S. The renaissance of GSK3. Nat Rev Mol Cell Biol 2001; 2:769-76; PMID:11584304; https://doi.org/10.1038/35096075

[42] Roux KJ, Kim DI, Raida M, Burke B. A promiscuous biotin ligase fusion protein identifies proximal and interacting proteins in mammalian cells. J Cell Biol 2012; 196:801-10; PMID:22412018; https://doi.org/10.1083/jcb.201112098

[43] Roux KJ, Kim DI, Burke B. BioID: a screen for protein-protein interactions. Curr Protoc Protein Sci 2013; 74: Unit 19 23; PMID:24510646; https://doi.org/10.1002/0471140864.ps1923s74

[44] Suter DM, Forscher P. Transmission of growth cone traction force through apCAM-cytoskeletal linkages is regulated by Src family tyrosine kinase activity. J Cell Biol 2001; 155:427-38; PMID:11673478; https://doi.org/10.1083/jcb.200107063

[45] Scheid MP, Woodgett JR. PKB/AKT: functional insights from genetic models. Nat Rev Mol Cell Biol 2001; 2:760-8; PMID:11584303; https://doi.org/10.1038/35096067

[46] Hers I, Vincent EE, Tavare JM. Akt signalling in health and disease. Cell Signal 2011; 23:1515-27; PMID:21620960; https://doi.org/10.1016/j.cellsig.2011.05.004

[47] Seo KW, Lee SJ, Kim YH, Bae JU, Park SY, Bae SS, Kim CD. Mechanical stretch increases MMP-2 production in vascular smooth muscle cells via activation of PDGFR-beta/Akt signaling pathway. PloS One 2013; 8:e70437; PMID:23950935; https://doi.org/10.1371/journal.pone.0070437

[48] Liu X, Huang X, Chen L, Zhang Y, Li M, Wang L, Ge C, Wang H, Zhang M. Mechanical stretch promotes matrix metalloproteinase-2 and prolyl-4-hydroxylase alpha1 production in human aortic smooth muscle cells via Akt-p38 MAPK-JNK signaling. Int J BiochemCell Biol 2015; 62:15-23; https://doi.org/10.1016/j.biocel.2015.02.009

[49] Qi Y, Li Z, Kong CW, Tang NL, Huang Y, Li RA, Yao X. Uniaxial cyclic stretch stimulates TRPV4 to induce realignment of human embryonic stem cell-derived cardiomyocytes. J Mol Cell Cardiol 2015; 87:65-73; PMID:26259779; https://doi.org/10.1016/j.yjmcc.2015.08.005

[50] Zhang B, Peng F, Wu D, Ingram AJ, Gao B, Krepinsky JC. Caveolin-1 phosphorylation is required for stretch-induced EGFR and Akt activation in mesangial cells. Cell Signal 2007; 19:1690-700; PMID:17446044; https://doi.org/10.1016/j.cellsig.2007.03.005

[51] Zeller KS, Riaz A, Sarve H, Li J, Tengholm A, Johansson S. The role of mechanical force and ROS in integrin-dependent signals. PloS One 2013; 8:e64897; PMID:23738008; https://doi.org/10.1371/journal.pone.0064897

[52] Sawada Y, Sheetz MP. Force transduction by Triton cytoskeletons. J Cell Biol 2002; 156:609-15; PMID:11839769; https://doi.org/10.1083/jcb.200110068

[53] Mohamed JS, Lopez MA, Boriek AM. Mechanical stretch up-regulates microRNA-26a and induces human airway smooth muscle hypertrophy by suppressing glycogen synthase kinase-3beta. J Biol Chem 2010; 285:29336-47; PMID:20525681; https://doi.org/10.1074/jbc.M110.101147

[54] Benham-Pyle BW, Pruitt BL, Nelson WJ. Cell adhesion. Mechanical strain induces E-cadherin-dependent Yap1 and beta-catenin activation to drive cell cycle entry. Science 2015; 348:1024-7; PMID:26023140; https://doi.org/10.1126/science.aaa4559

[55] Wang JG, Miyazu M, Matsushita E, Sokabe M, Naruse K. Uniaxial cyclic stretch induces focal adhesion kinase (FAK) tyrosine phosphorylation followed by mitogen-activated protein kinase (MAPK) activation. Biochem Biophys Res Commun 2001; 288:356-61; PMID:11606050; https://doi.org/10.1006/bbrc.2001.5775

[56] Hirata H, Gupta M, Vedula SR, Lim CT, Ladoux B, Sokabe M. Actomyosin bundles serve as a tension sensor and a platform for ERK activation. EMBO Reports 2015; 16:250-7; PMID:25550404; https://doi.org/10.15252/embr.201439140

[57] Hirata H, Sokabe M. A novel role of actomyosin bundles in ERK signaling. Commun Integr Biol 2015; 8:e1017176; https://doi.org/10.1080/19420889.2015.1017176